

Fast and stable predictions of material properties of solid solution alloys

Massimiliano Lupo Pasini¹, Ying Wai Li², Junqi Yin³, Jiaxin Zhang⁴, Kipton Barros⁵ and Markus Eisenbach³

¹ Oak Ridge National Laboratory, Computational Sciences and Engineering Division, Oak Ridge, TN 37831

² Los Alamos National Laboratory, Computer, Computational and Statistical Sciences Division, Los Alamos, NM 87545

³ Oak Ridge National Laboratory, National Center for Computational Sciences, Oak Ridge, TN 37831

⁴ Oak Ridge National Laboratory, Computer Science and Mathematics Division, Oak Ridge, TN 37831

⁵ Los Alamos National Laboratory, Physics and Chemistry of Materials, Theoretical Division, Los Alamos, NM 87545

E-mail: lupopasini@ornl.gov, eisenbachm@ornl.gov

Abstract. We present a deep learning approach to produce highly accurate predictions of macroscopic physical properties of solid crystals. Since the distribution function of the total energy would enable a thorough understanding of the macroscopic properties for alloys and magnetic systems, surrogate deep learning models can replace first principle calculations to speed up each sample from the total energy distribution function. However, neural network models lose accuracy with respect to first principle calculations and this affects the reliability of the estimate. Here, we focus on reducing the uncertainty of multitasking neural network models to simultaneously predict physical properties of alloys. The uncertainty is reduced relying on the physical correlation of the magnetic moment with total energy and charge density. These physical quantities mutually serve as constraints during the training of the multitasking deep learning model, which leads to more reliable deep learning models because the physics is also learned correctly. We present numerical experiments for two types of binary alloys: copper-gold and iron-platinum. The dataset comprises information about total energy, charge density and magnetic moment (for magnetizable materials) computed via first principle codes for 32,000 configurations which differ per composition to properly span the entire state space. The training of the neural network is performed using 90% of the dataset, whereas the remaining 10% is used to test the predictive performance of the deep learning model. Results show that multitasking neural networks estimate the material properties for a specific state space hundreds of times faster than the first principle codes used as a reference. Moreover, the inclusion of the magnetic moment as a physical constraint for iron-platinum significantly reduces the uncertainty of the predictions by damping the fluctuations of the predictive performance with respect to different validation splittings of the dataset.

This manuscript has been authored in part by UT-Battelle, LLC, under contract DE-AC05-00OR22725 with the US Department of Energy (DOE). The US government retains and the publisher, by accepting the article for publication, acknowledges that the US government retains a nonexclusive, paid-up, irrevocable, worldwide license to publish or reproduce the published form of this manuscript, or allow others to do so, for US government purposes. DOE will provide public access to these results of federally sponsored research in accordance with the DOE Public Access Plan (<http://energy.gov/downloads/doe-public-access-plan>).

Introduction

Understanding and controlling the properties of materials at different structural levels is essential for technological progress. However, modeling the behavior of matter at the atomic and molecular level is extremely challenging.

Several computational approaches have been developed through the past decades to model and predict the quantum behavior of atoms and molecules. In particular, first principles methods such as Density Functional Theory (DFT) [16, 19, 17], Quantum Monte Carlo (QMC) [21, 13] and *ab-initio* Molecular Dynamics (MD)[10, 1, 22] have shed new light into the understanding of materials at atomic and molecular scale. In fact, these techniques combined with importance-sampling algorithms [14] can reconstruct the entire probability distribution of the total energy of a solid crystal at a fixed temperature to obtain a complete understanding of the macroscopic physical properties of a material. However, first principle computations of the total energy distribution become computationally unpractical as the system size increases, because computing the total energy for each configuration needs numerical integrations in a high dimensional domain. An opportunity to reduce the computational time is offered by algorithms that can be used to build inexpensive surrogate neural network models to replace expensive first principle calculations [15]. Indeed, deep learning models [20, 3] are flexible in terms of range of applications and adjustable computational complexity and several studies have already explored how neural networks can benefit electronic structure and molecular dynamics calculations [4, 31, 27, 6, 25]. However, the estimation of the total energy needs to be highly accurate in order for the the importance-sampling to properly reconstruct the probability distribution on the entire state space. Therefore, stringent requirements on the predictive performance of the neural network must be imposed.

The goal of this work is to replace expensive direct calculations with highly accurate and computationally inexpensive deep learning models to compute the energy of a solid crystal lattice configuration, which is needed for each step of the importance-sampling algorithm to estimate the total free energy distribution function. In particular, we focus on solid structures related to binary alloys and magnetic systems. The quantities computed with the forward code via first principle calculations are employed to generate the dataset for the training of the neural networks. The output of first principle calculations is treated as the exact reference point and the departure from the first principle calculations is used to assess the performance of the deep learning models. Although the total energy is the main macroscopic quantity of interest for the study of statistical mechanics, other microscopic quantities such as charge distribution and atomic magnetic moment can be sometimes object of research as well. To this goal, the joint training [5] can be used to simultaneously predict multiple physical quantities by using multi-tasking neural networks. For the goal of this work, we require the neural network to simultaneously predict the total energy, the charge density and the magnetic moment (when this is possible) of each atom in the lattice. In order to improve the predictive performance of multi-tasking neural network models we aim to reduce the uncertainty of the predictions generated and we achieve so by identifying the physical quantities that are stronger correlated to each other and use these as mutual constraints during the joint training. The numerical experiments presented in this paper show that neural networks can significantly reduce the computational time to estimate the macroscopic physical properties of a material compared to forward codes. Moreover, we show that the use of the magnetic moment as a physical constraint can reduce the uncertainty for the predictions of total energy and charge density with respect to situations where the magnetic moment is not included as a physical constraint for the joint training.

This paper is organized in four sections. Section 1 describes the Physics background, Section 2 describes the main properties of neural networks, Section 3 shows numerical experiments for the copper-gold and iron-platinum binary alloys and Section 4 summarizes the results presented and explains possible future directions to continue the research in this field.

1. Physical system - binary alloys

The model systems we analyze are binary alloys. Specifically, we focus on solid solution alloys, where the constituent atoms are placed on a fixed underlying crystal lattice that does not change with the composition of the alloy. We use density functional theory (DFT) with a multiple scattering approach implemented in LSMS [7, 28] as a reference for first principle calculations to compute energy, charge density and magnetic moment of alloys. The ultimate goal of our research is the understanding of the thermodynamics and of phase transitions in alloys. The evaluation of these properties relies on the calculation of the partition function $Z(T)$ of the system

$$Z(T) = \sum_{\mathbf{x}} e^{H(\mathbf{x})/k_B T}$$

where T is the temperature and k_B the Boltzmann constant. The summation is over all possible configurations \mathbf{x} of the system. The Hamiltonian $H(\mathbf{x})$ represents the energy of the alloy system associated with the atom configuration \mathbf{x} . For details of the relation of $Z(T)$ to the thermodynamic behavior of alloys and how to efficiently evaluate it are topics beyond the scope of the present paper and can be found in [9] and references therein.

The focus of the present paper is the efficient and reliable evaluation of the Hamiltonian of the system. The main computational complexity of calculating the energy of a system of atoms within DFT arises from the iterative solution of the Kohn-Sham equation

$$\left(-\frac{\hbar}{2m} \nabla^2 + V_{ext}(\mathbf{r}; \mathbf{x}) + v_{xc}[\rho(\mathbf{r})](\mathbf{r}) \right) \psi_i(\mathbf{r}) = \epsilon_i \psi_i(\mathbf{r})$$

where the external potential V_{ext} depends on the chemical composition of the alloy under consideration and the electron density enters the exchange correlation potential v_{xc} , thus creating a dependence on the Kohn-Sham orbitals ψ_i . Within this scheme, the process to compute the ground state energy of an alloy system with the first principle code can be summarized through the following steps:

- (i) provide a lattice configuration with information about the Cartesian coordinates of each atom in the lattice and the atom species at each location
- (ii) set up an initial guess for the electron density
- (iii) perform self-consistent iterations to iteratively update the electron density by solving the Kohn-Sham equations
- (iv) use the iteratively updated individual electron wave functions resulting from the converged self-consistent iteration to compute the ground state electron density
- (v) evaluate the energy functional at the ground state electron density to compute the ground state energy

The computational requirements and time to perform these steps are challenging even for state-of-the-art high performance computing architectures when the lattice contains thousands of atoms, even using our highly scalable LSMS method. Therefore, deep learning models provide an alternative as surrogates models to expedite the estimation of the ground state energy for a given lattice configuration.

The use of a properly trained neural network to estimate the total energy of a solid crystal configuration would allow us to directly connect steps 1 and 5 without the need to perform the intermediate steps 2-4.

2. Deep feedforward networks

A deep feedforward network, also called feedforward neural network, or multilayer perceptron (MLP) [23, 12] is a predictive statistical model to approximate some unknown function f of the form

$$y = f(x),$$

where $x \in \mathbb{R}^a$, $y \in \mathbb{R}^b$ and $f : \mathbb{R}^a \rightarrow \mathbb{R}^b$. Given a collection of m vectors for x stored in $\mathbf{x} \in \mathbb{R}^{am}$ and the corresponding m vectors of $f(x)$ stored in $\mathbf{y} = f(\mathbf{x}) \in \mathbb{R}^{bm}$, feedforward neural networks search a mapping that approximates to the best the unknown function f . Indeed, feedforward neural networks compose together many different functions such as

$$\hat{f}(x) = f_\ell(f_{\ell-1}(\dots f_0(x))), \quad (1)$$

where $\hat{f} : \mathbb{R}^a \rightarrow \mathbb{R}^b$, $f_0 : \mathbb{R}^a \rightarrow \mathbb{R}^{k_1}$, $f_\ell : \mathbb{R}^{k_\ell} \rightarrow \mathbb{R}^b$ and $f_p : \mathbb{R}^{k_p} \rightarrow \mathbb{R}^{k_{p+1}}$ for $p = 1, \dots, \ell - 1$. The goal is to identify the proper number ℓ so that the composition in Equation (1) resembles the unknown function f . The composition in Equation (1) is modeled via a directed acyclic graph describing how the functions are composed together. The number ℓ that quantifies the complexity of the composition is equal to the number of hidden layers in the neural network. Therefore, f_1 corresponds to the first layer of the neural network, f_2 is the second layer and so on. In other words, deep feedforward networks are nonlinear regression models and the nonlinearity is given by the composition in Equation (1) used to model the relation between input data x and output y .

This approach can be reinterpreted as searching for a mapping that minimizes the discrepancy between values $\mathbf{y}_{\text{predicted}}$ predicted by the model and given observations \mathbf{y} . The behavior and the complexity of a statistical model is controlled by a set of parameters that we represent as $\mathbf{w} \in \mathbb{R}^N$, where N is the dimensionality of the parameter space. Given a dataset with m data points, the process of predicting the outputs for given inputs via a feedforward neural network can thus be formulated as

$$\mathbf{y}_{\text{predicted}} = F(\mathbf{x}, \mathbf{w}), \quad (2)$$

where

- $\mathbf{x} \in \mathbb{R}^{am}$ is the vector of inputs
- $\mathbf{w} \in \mathbb{R}^N$ is the vector of parameters describing the feedforward neural network
- $F : \mathbb{R}^{am \times N} \rightarrow \mathbb{R}^{bm}$ is the forward operator
- $\mathbf{y}_{\text{predict}} \in \mathbb{R}^{bm}$ is the vector of the predicted output via the forward operator F

The goal is to learn the value of the parameters \mathbf{w} corresponding to the best approximation of f . The quality of an approximation and thus the selection of one as best depends on the optimality criterion adopted to discriminate the performance of each neural network. The optimality criterion to select the parameters \mathbf{w} usually consists of minimizing the discrepancy between given observations \mathbf{y} and predicted output $\mathbf{y}_{\text{predicted}}$ as follows:

$$\mathbf{w}_{\text{opt}} = \underset{\mathbf{w} \in \mathbb{R}^N}{\text{argmin}} \quad \|\mathbf{y} - \mathbf{y}_{\text{predicted}}(\mathbf{w})\|_2, \quad (3)$$

where $\|\cdot\|_2 : \mathbb{R}^{bm} \rightarrow \mathbb{R}^+$ represents the Euclidean norm in \mathbb{R}^{bm} . In this paper, we consider y as the total energy of a solid crystal at the ground state.

As any other statistical model used for predictive purposes, feedforward neural networks can incur overfitting. The term overfitting generally refers to numerical artifacts that make the predictive model

extremely accurate on data it was trained on but extremely inaccurate on new data samples. Several techniques have been proposed to cope with this numerical problem. The most generic approaches are the control of the computational complexity of the model and regularization on the parameters. The former consists of capping the dimensionality of the parameter space so that the complexity of the predictive model does not exceed what is justified by the amount of data available. The latter consists of reinterpreting a constrained optimization problem as a penalized global optimization problem, where the new objective function is the sum of the old objective function and an additional term that enforces the constraint in a weak form via Lagrange multipliers.

2.1. Regularization techniques

We consider a regularization technique where the constraint is expressed in terms of quantities that are descriptive of the physics for the solid crystal structures. In particular, we adopt charge density and/or magnetic moment as constraint on the prediction of the total energy.

Therefore, the constrained optimization problem related to a regularization technique can be expressed as

$$\begin{cases} \min_{\mathbf{w}} & \|\mathbf{y} - \mathbf{y}_{\text{predicted}}(\mathbf{w})\|_2 \\ \mathbf{c}(\mathbf{w}) = \mathbf{g} \end{cases}, \quad (4)$$

where $\mathbf{w} \in \mathbb{R}^N$ is the vector of parameters of the model and $\mathbf{c}(\mathbf{w}) \in \mathbb{R}^c$ and $\mathbf{g} \in \mathbb{R}^c$ are quantities used to express a constraint. For the scope of this paper, we consider a regularization technique where $\mathbf{c}(\mathbf{w})$ and \mathbf{g} are closely related to the electronic properties of solid crystal structures. In particular, we will choose \mathbf{g} as charge density and/or magnetic moment computed via DFT calculations and $\mathbf{c}(\mathbf{w})$ represents their prediction computed via neural networks. The formulation in (4) imposes the constraint $\mathbf{c}(\mathbf{w}) = \mathbf{g}$ in a strong form. The values of $\mathbf{c}(\mathbf{w})$ depend on the model configuration identified by the parameter vector \mathbf{w} , whereas the values of \mathbf{g} are assumed to be given.

The objective function in (4) can be modified so that the constraint is incorporated in the definition of the objective function itself as follows:

$$\|\mathbf{y} - \mathbf{y}_{\text{predicted}}(\mathbf{w})\|_2 + \lambda \|\mathbf{c}(\mathbf{w}) - \mathbf{g}\|_2, \quad (5)$$

The objective function minimized in (5) is a the result of interpreting the constraint as a penalization term, since the penalization multiplier λ tunes a weak formulation of the constraint that is added as an extra term in the original objective function. Therefore, the constraint optimization problem (4) can be reformulated as

$$\min_{\mathbf{w}} \left\{ \|\mathbf{y} - \mathbf{y}_{\text{predicted}}(\mathbf{w})\|_2 + \lambda \|\mathbf{c}(\mathbf{w}) - \mathbf{g}\|_2 \right\}, \quad (6)$$

which is a global optimization problem. An alternative way to interpret (6) is to train a neural network on multiple quantities. Each predicted quantity is associated with a loss function. Therefore, the global objective function minimized by the training of the neural network is a linear mixing of the individual loss functions. This approach is called *multi-tasking learning* or *joint training*.

2.2. Multi-tasking learning or joint training

Multi-tasking learning (MTL), also known as joint training, was initially introduced by R. A. Caruana [5] to extend the utilization of a neural network to simultaneously predict multiple quantities. The rationale

is that predicted quantities could play as an inductive bias for each other, leading the learning model to prefer some hypotheses over others. In other words, the MTL is expected to retain information that can benefit multiple tasks altogether rather than a specific one. The strength of an MTL model depends on how tasks are related. In this paper we focus on MTL models that are field specific, meaning that the tasks are drawn from the same domain. This type of field specific inductive bias has been defined as *knowledge-based*, meaning that a task can benefit from the information contained in the training signal for other tasks. Indeed, the other tasks can provide additional domain knowledge that could not be used if the tasks were executed independently from each other. Therefore, every single task is treated as an enrichment of the knowledge available to train other domain specific quantities of interest. In Figure 1 we show the topology of four neural networks to model four distinct functions on the same input, whereas Figure 2 shows the topology of a neural network for multi-tasking learning to model four related functions defined on the same inputs. The architecture of the neural network for MTL is organized so that the hidden layers are shared between all tasks, while keeping several task-specific output layers. This approach is known in literature as *hard parameter sharing*.

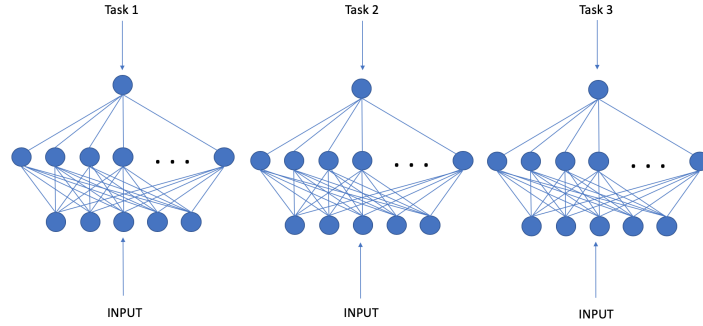


Figure 1. Topology of neural networks for Single Task Learning (STL) of four functions defined on the same inputs

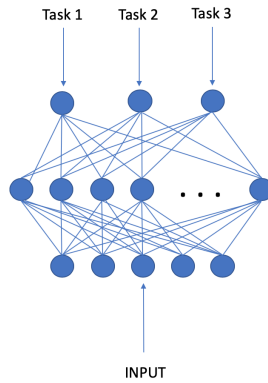


Figure 2. Topology of a neural network for Multitask Learning (MTL) of four related functions defined on the same inputs

Let us refer to T as the total number of tasks we want to predict. A single task identified by index i focuses on reconstructing a function $f_i : \mathbb{R}^a \rightarrow \mathbb{R}^{b_i}$ defined as

$$y_i = f_i(x), \quad i = 1, \dots, T \quad (7)$$

where $x \in \mathbb{R}^a$, $y_i \in \mathbb{R}^{b_i}$. The multitask learning aims to exploit the relation between the quantities y_i 's so that the functions in (7) could be replaced by a single function $\hat{f} : \mathbb{R}^a \rightarrow \mathbb{R}^{\sum_i^T b_i}$ that can model all the relations between inputs and outputs as follows:

$$\begin{bmatrix} y_1 \\ \vdots \\ y_T \end{bmatrix} = \hat{f}(x). \quad (8)$$

As in Section 2, we assume that the training dataset contains m data points. Therefore, each task needs to reconstruct the function f_i by associating a vector of m inputs (denoted as $\mathbf{x} \in \mathbb{R}^{am}$) with a vector of m outputs (denoted as $\mathbf{y} \in \mathbb{R}^{m \sum_i^T b_i}$).

We refer to N_{MTL} as the total number of weights used by the neural network for the MTL. The goal of MTL is to look for a function \hat{f} described as in (8). Therefore, the forward operator $F_{MTL} : \mathbb{R}^{am} \times \mathbb{R}^{N_{MTL}} \rightarrow \mathbb{R}^{m \sum_i^T b_i}$ to predict the outputs with the the neural network is

$$[\mathbf{y}_1, \dots, \mathbf{y}_T] = F_{MTL}(\mathbf{x}, \mathbf{w}_{MTL}),$$

where

- $\mathbf{x} \in \mathbb{R}^{am}$ is the vector of inputs
- $\mathbf{w}_{MTL} \in \mathbb{R}^{N_{MTL}}$ is the vector of weights for the multi-tasking neural network
- $F : \mathbb{R}^{am \times N_{MTL}} \rightarrow \mathbb{R}^{m \sum_i^T b_i}$ is the forward operator for the multi-tasking learning
- $\mathbf{y}_i \in \mathbb{R}^{mb_i}$ (for $i = 1, \dots, T$) is the vector of outputs for the i th quantity of interest

The loss function $\ell_{MTL} : \mathbb{R}^{N_{MTL}} \rightarrow \mathbb{R}^+$ minimized in MTL is a linear combination of the loss functions for the single tasks, such that

$$\ell_{MTL}(\mathbf{w}_{MTL}) = \sum_{i=1}^T \alpha_i \|\mathbf{y}_i - \mathbf{y}_{predict,i}(\mathbf{w}_{MTL})\|_2, \quad (9)$$

where

- T is the total number of tasks for the MTL approach
- $\mathbf{w}_{MTL} \in \mathbb{R}^{N_{MTL}}$ is the vector containing all the weights across the entire neural network
- $\mathbf{y}_{predict,i} \in \mathbb{R}^{mb_i}$ (for $i = 1, \dots, T$) is the vector of predictions for the i th quantity of interest
- α_i (for $i = 1, \dots, T$) are the mixing weights for the loss functions $dist_i$'s

As we already mentioned earlier, the MTL can be interpreted as an inductive bias because the loss function of a quantity operates as a regularizer with respect to the loss functions of the other quantities predicted.

3. Numerical implementation

In this section we present numerical experiments to assess the computational time reduction obtained through surrogate deep learning models as a replacement of first principle codes to estimate macroscopic physical properties (e.g. total energy, charge density and magnetic moment) for lattice configurations of binary alloys and magnetic systems. In addition, we measure the uncertainty of the predictions generated by the joint training when multiple quantities simultaneously predicted using multi-tasking neural networks and we compare it with the uncertainty of standard neural networks trained on single quantities.

3.1. Description of test cases

We consider two test cases associated with two binary alloy systems with regular cubic structures. The first numerical test considers a copper-gold (CuAu) alloy with 32 atoms located in a face-centered cubic (FCC) structure and the second numerical test considers an iron-platinum (FePt) alloy with 32 atoms located in a body-centered cubic (BCC) structure. For both test cases, only 32,000 configurations are extracted out of the total 2^{32} configurations available to create the dataset. The copper-gold binary alloy is a non magnetizable alloy and each data point in the dataset provides the information of a specific lattice configuration with the total energy and the charge density. The iron-platinum alloy has magnetic properties and each data point in the dataset contains information about a specific lattice configuration, the charge density and the magnetic moment as well. The dataset for each material comprises several lattice configurations for each composition (percentage of atom species in the compound). The selection of the configurations is performed to ensure that every composition is equally represented in the dataset. The proper representation of each composition is guaranteed according to the following approach: if the configurations for a specific composition are less than 1,000, then every possible configuration is included in the dataset; otherwise 1,000 configurations are randomly selected among all the possible configurations that the specific composition allows. Although the change of composition may induce the crystal to change the type of cubic structure to reach a lower energy state in nature, the underlying structure is fixed across different compositions for the experiments we perform here. A possible change of cubic structure in an alloy due to different composition would require the deep learning model to treat the geometric structure as an extra parameter. However, the parametrization of the geometric structure is not addressed in this work. The physical quantities for each selected configuration are computed with a locally self-consistent multiple scattering (LSMS) method [28]. The code employed to perform the LSMS calculations is the LSMS-3 code implemented at Oak Ridge National Laboratory [8]. In terms of units, the total energy is measured in Rydberg, the atomic charge is measured in electron units and the atomic magnetic moment is measured in Bohr magnetons.

3.2. Set-up of statistical models

As for the copper-gold test case, the single-tasking neural networks are made of two hidden layers and each hidden layer contains 200 nodes, whereas the multi-tasking neural networks are made of three hidden layers. The first two hidden layers in multi-tasking neural networks have 200 nodes that are shared across all the tasks, whereas the last hidden layer is task-specific. The total number of nodes in the task-specific hidden layer is still 200, but these are equally split across the two tasks to predict total energy and charge-density. The loss functions associated with each predicted quantity are linearly mixed to create a global objective function that is minimized through the joint training. The mixing weights are currently hand-tuned with a trial and error approach. In particular, the weights α_i 's used for the loss functions are 0.0001 for total energy and 8.0 for the charge density. The difference in orders of magnitude between the loss function weights compensates the difference in orders of magnitude between the physical quantities predicted. In fact, the total energy is of the order of hundreds of thousands of Rydberg, whereas the atomic charge is quantified in electron units.

As for the iron-platinum test-case, the single-tasking neural networks are made of two hidden layers and each hidden layer contains 300 nodes. The neural network for multi-tasking is made of three hidden layers. The first two hidden layers have 300 nodes each and they are shared across all the tasks, whereas the last hidden layer is task-specific. The total number of nodes in the the task-specific hidden layer is 300, but these nodes are equally split for each task. The possible targets that a deep learning model can predict

in this case are total energy, charge density and magnetic moment. The presence of the magnetic moment as an additional quantity increases the number of ways that the physical quantities can be combined for the joint training. Also in this case, the mixing coefficients α_i 's for the loss functions counterbalance the difference in orders of magnitude between the physical quantities acting as mutual constraints for the joint training.

For the neural network predicting simultaneously all the three quantities, the weights α_i 's used for the loss functions are 0.0001 for total energy, 70.0 for the charge density and 1.0 for the magnetic moment. For the neural network predicting simultaneously total energy and charge density, the weights α_i 's used for the loss functions are 0.0001 for total energy and 8.0 for the charge density. For the neural network predicting simultaneously total energy and magnetic moment, the weights α_i 's used for the loss functions are 0.0001 for total energy and 8.0 for the magnetic moment. For the neural network predicting simultaneously charge density and magnetic moment, the weights α_i 's used for the loss functions are 1.7 for charge density and 1.0 for the magnetic moment.

The regression weights of the neural networks are optimized with the Adam method [18] with an initial learning rate equal to 0.0001. The total number of epochs performed is 30,000 and the batch for each step of an epoch is 10% of the training set.

3.3. Comparison between computational times for first principle calculations and deep learning models

In this section we compare the time needed to estimate the total energy for a lattice configuration using first principle calculations, single-tasking neural networks and multi-tasking neural networks for copper-gold and iron-platinum. The output of DFT calculations is considered as the exact quantity that the deep learning model has to reconstruct. Therefore, the predictive performance of a deep learning model is tested by measuring the departure of quantities predicted with deep learning models from the results produced by DFT calculations. The first principle calculations are performed with the LSMS-3 code on the Titan supercomputer at Oak Ridge National Laboratory using 8 physical cores for an hybrid MPI-CUDA parallelization. For more details about the hardware specifics of Titan we refer to [30]. The training and testing of the neural networks are performed on a personal laptop and the training is stopped when the validation error is below 0.01/Results for the two binary alloys are shown in tables 1 and 2 respectively. Significant time reductions are obtained for both the test cases when neural networks are used in place of state-of-the-art first principle calculations. Indeed, first principle calculations take about 480 wall-clock seconds on average for copper-gold and 530 for iron-platinum, whereas the neural networks predict the physical quantities in about a wall-clock second. The wall-clock times presented in Tables 1 and 2 for the neural networks do not account for the computational time spent to train the deep learning models. The training of the neural networks takes between 10,000 to 20,000 wall-clock seconds on a laptop according to the number of quantities that the neural network is trained on, since this affects the complexity of the objective function to minimize. The results in Tables 1 and 2 thus show that a trained neural network can significantly reduce the computation time with respect to first principle calculations and still produce highly accurate estimates for the physical quantities of interest.

3.4. Comparison between statistical models for predictive performance

In this section we compare the performance of neural networks trained on a single task and the performance of neural networks trained on multiple tasks. The output of DFT calculations are used as reference values. Therefore, the predictive performance of neural network models measures the departure of values predicted with deep learning approaches from the first principle calculations that are treated as exact. The results

Computational approach	Wall-clock time(s)
first principle calculation	480.1
single-tasking neural network	0.8
multi-tasking neural network	0.9

Table 1. CuAu binary alloy - Average time in wall-clock seconds needed to estimate macroscopic physical properties on a random lattice configuration with first principle calculations, single-tasking neural networks, and multi-tasking neural networks.

Computational approach	Wall-clock time(s)
first principle calculation	530.2
single-tasking neural network	0.9
multi-tasking neural network	1.1

Table 2. FePt binary alloy - Average time in wall-clock seconds needed to estimate physical properties on a random lattice configuration with first principle calculations, single-tasking neural networks, and multi-tasking neural networks.

are produced with neural networks with a fixed architecture, opposed to the analysis in [5] where neural networks with different sizes were considered. The fixed size for the architecture of a neural network is an insightful approach for the goal of this work. In fact, this approach forces small multi-tasking neural networks to find a joint function to predict all the quantities, as opposed to big networks where multiple independent functions are represented through different regions of the neural network. The performance of neural networks is compared with the XGBoost algorithm [32]. More specifically, the Python API implementation of XGBoost [33] with a default set-up for hyper parameters is employed. For further details about the default hyper parameter values we refer to the documentation in [33].

The performance is measured by monitoring the regression score for the predictions on the test set and the uncertainty associated with the predictions is quantified through the standard deviation. The regression score, also known as R^2 or coefficient of determination, is defined as

$$R^2 = 1 - \frac{\sum_{i=1}^N \|\mathbf{y}_i - \hat{\mathbf{y}}_i\|_2^2}{\sum_{i=1}^N \|\mathbf{y}_i - \bar{\mathbf{y}}\|_2^2}, \quad (10)$$

where $\{\mathbf{y}_i\}_{i=1}^N$ are the observations, $\{\hat{\mathbf{y}}_i\}_{i=1}^N$ are the predictions generated with the model, $\bar{\mathbf{y}} = \frac{1}{N} \sum_{i=1}^N \mathbf{y}_i$ is the sample mean and $\|\cdot\|_2$ is the Euclidean norm, whereas the standard deviation for one dimensional observations $\{y_i\}_{i=1}^N$ with sample mean \bar{y} is defined as

$$\sigma = \sqrt{\frac{1}{N-1} \sum_{i=1}^N (y_i - \bar{y})^2}. \quad (11)$$

The results are averaged over 60 runs that differ from each other by shuffling the split of the dataset between training and testing portions. Table 3 and 4 show the sample mean and the standard deviation of the test regression score for each physical quantity predicted by the neural networks. The sample mean of the test regression score provides a point-wise estimation of the predictive power of the model, whereas the standard deviation quantifies the reliability of the test score in effectively describing the predictive

performance of the model. Statistical models with a regression score closer to the unit from below are to be interpreted as better performing and smaller values of the standard deviation are to be interpreted as a more reliable quantification of the predictive performance of the model. The name of each row in the tables refers to either multi-tasking or single-tasking neural networks and the capital letters are associated with the quantities predicted (E stands for total energy, C stands for charge density and M stands for magnetic moment). Since the architecture of the neural networks is fixed, the regression score for multi-tasking neural networks may decrease with respect to single-tasking neural networks, as the same amount of computational resources is shared among multiple quantities to be predicted. In traditional studies involving machine learning, the performance of a model would be measured by its level of generalizability in retaining relevant features of the dataset and therefore accurately estimating the output for inputs outside the training range. This translates into the property of the model to avoid overfitting, which is usually diagnosed by a training error much lower than the validation error. However, we want to emphasize that we adopt a more global concept of predictive performance of a model. We actually aim to show that our entire procedure leads to a more generalizable model, regardless of the specific dataset adopted for the training. To this goal, we do not look at the error of a single model, because our claim does not aim to show just that a single model is generalizable. In our case, the effectiveness of the joint training in stabilizing the predictions is assessed through the standard deviation of the regression score as a metric of the uncertainty associated with the predictions. Indeed, the more a prediction is stable, the more likely the accuracy attained by the model is independent of the specific portion of dataset used for the training of the model itself. Therefore, more robust and stable models should lead to lower values of standard deviation for the regression score. If the joint training causes the regression score to decrease and the standard deviation to increase at the same time, this means that the quantities predicted are weakly correlated.

With regards to the copper-gold test case, a loss in precision is noticed when total energy and charge density are predicted simultaneously versus predicting them one at a time. Indeed, results in Table 3 show a decrease of the regression score along with a significant increase in the standard deviation for multi-tasking neural networks. The increase of the standard deviations for the regression score means that the predictions are more prone to fluctuations due to the shuffling of the dataset, making the outcome of the predictive model less stable and less reliable. This outcome suggests that total energy and charge density are weakly correlated, causing the total energy and charge density to compete against each other for the contention of computational resources inside the multi-tasking neural network. The explanation seems to be confirmed by the outcome of the iron-platinum test case in Table 4 for the same type of joint training that involves total energy and charge density. Indeed, the neural network model that simultaneously predicts total energy and charge density is still less precise than the ones employed for single predictions and the loss of accuracy is still accompanied by a higher value of the standard deviation. However, the magnetic moment can be included in the multi-tasking learning because iron-platinum is a magnetizable alloy. From the distribution of computational resources, one would expect that adding the magnetic moment would worsen even more the predictions because the same computational resources are now to be split across more targets. However, the numerical experiments in Table 4 counterintuitively show that adding the magnetic moment as a physical constraint improves the predictive performance of multi-tasking neural networks. In fact the regression scores for the total energy and charge density benefit from the inclusion of the magnetic moment as a constraint. This is also validated by a significant reduction of the standard deviations, meaning that the predictions are more stable. A plausible explanation for these results is that the correlation between total energy and magnetic moment is stronger than the correlation between total energy and charge density. The idea that multi-tasking learning can produce more physically reliable

predictions is also supported by laboratory experiments, where a stronger correlation between energy and magnetic moment than between energy and charge density has been noticed.

Dataset	Total Energy		Charge density	
	Mean	St. dev.	Mean	St. dev.
multi-tasking_EC	0.999990	6.164184e−6	0.990106	0.008903
single-tasking_E	0.999999	1.147116e−7	-	-
single-tasking_C	-	-	0.993889	0.002019

Table 3. CuAu binary alloy - Mean value and standard deviation for test regression score over 60 runs. Each run performs the training of multi-tasking and single-tasking neural networks to predict total energy and charge density.

Dataset	Total Energy		Charge density		Magnetic moment	
	Mean	St. dev.	Mean	St. dev.	Mean	St. dev.
mukltitasking_ECM	0.999976	4.599659e−6	0.976299	0.009010	0.990846	0.003747
multi-tasking_EC	0.999989	5.277086e−6	0.959282	0.021857	-	-
multi-tasking_EM	0.999985	3.321548e−5	-	-	0.974768	0.033481
multi-tasking_CM	-	-	0.978824	0.004639	0.996109	0.000824
single-tasking_E	0.999999	1.147116e−7	-	-	-	-
single-tasking_C	-	-	0.993889	0.002019	-	-
single-tasking_M	-	-	-	-	0.996505	0.000884

Table 4. FePt binary alloy - Mean value and standard deviation for test regression score for 60 runs. Each run performs the training of multi-tasking and single-tasking neural networks to predict total energy, charge density and magnetic moment.

4. Conclusions and future developments

In this paper we presented an approach to improve the reliability of neural network models when they are used to estimate macroscopic material properties of binary alloys as a replacement of first principle calculations. The approach resorts to a multitasking neural network model that is jointly trained on multiple quantities to reduce the uncertainty. Each predicted quantity acts as a physical constraint on the other quantities so that the reliability of the prediction is improved by enforcing the neural network model to retain information about the physical constraint. Numerical experiments for copper-gold and iron-platinum alloys are presented where material properties are estimated for systems of 32 atoms placed on regular cubic structures. The use of neural networks effectively reduces the time needed to derive the material properties by a factor of hundreds of wall-clock seconds compared to direct calculations. Improvements in the stability of the prediction have been obtained for the iron-platinum test case. In fact, the strong correlation of magnetic moment with the energy and the charge density of the material stabilizes the predictive performance in multi-tasking neural networks for all the targets predicted.

In the future, we would like to generalize the study by using convolutional neural networks (CNN) to capture local interactions between atoms. On the one hand, the use of CNN could reduce the computational cost to train the deep learning model with respect to fully connected neural networks. On other hand,

this would also make the deep learning model independent of the lattice size. Moreover, the use of graph convolutional neural networks may generalize the approach to simultaneously handle different geometries. When the volume of the data to handle is too large, an effective reduction of the size of the training set could be achieved either by constructing neural networks that automatically recognize crystal symmetries or by using reinforcement learning [24] to iteratively update the set-up of the neural network based on new data generated on the fly.

Acknowledgements

This work is supported in part by the Office of Science of the Department of Energy and by the LDRD Program of Oak Ridge National Laboratory. It used resources of the Oak Ridge Leadership Computing Facility, supported by the Office of Science of the U.S. Department of Energy, which is supported by the Office of Science of the U.S. Department of Energy under Contract No. DE-AC05-00OR22725.

References

- [1] Alder B J and Wainwright T E 1959 *Journal of Chemical Physics* **31** 459
- [2] Balabin R M and Lomakina I 2009 *Journal of Chemical Physics* **131** 074104
- [3] Bhadeshia H K D H 1999 *ISIJ International* **39** 966–979
- [4] Brockherde F, Vogt L, Li L, Tuckerman M E, Burke K and Müller K R 2017 *Nature Communications* **8** 872
- [5] Caruana R A 1997 *Multitask Learning* **28** 41–75
- [6] Custódio C A, Filletti É R and França V V 2019 *Scientific Reports* **9** 1886
- [7] Eisenbach M, Larkin J, Lutjens J, Rennich S and Rogers J H 2017 *Computer Physics Communications* bf 211 2–7
- [8] Eisenbach M, Li Y W, Liu X, Odbadrakh O K, Pei Z, Stocks G M and Yin J 2017 *LSMS. Computer software*, <https://www.osti.gov/servlets/purl/1420087>, Vers. 00, USDOE
- [9] Eisenbach M, Pei Z and Liu X 2019 *Journal of Physics: Condensed Matter* **31** 273002
- [10] Fermi E, Pasta J and Ulam S 1955 Los Alamos report LA-1940, 1955.
- [11] Gao T, Du J, Dai L and Lee C 2015 T. GAO, J. DU, L. DAI, AND C. LEE, *Joint training of front-end and back-end deep neural networks for robust speech recognition* 2015 IEEE International Conference on Acoustics, Speech, and Signal Processing (ICASSP)
- [12] Goodfellow I, Bengio Y and Courville A 2016 *Deep Learning*, (The MIT Press, Cambridge, Massachusetts)
- [13] Hammond B L, Lester W A and Reynolds P J 1994 *Monte Carlo Methods in Ab Initio Quantum Chemistry*, (Singapore: World Scientific)
- [14] Hastings W K 1970 *Biometrika* **57** 97–109
- [15] Haykin S 2009 *Neural Networks and Learning Machines, Third Edition*, (Prentice Hall, Pearson Education Ltd.)
- [16] Hohenberg P and Kohn W 1964 *Physical Review* **136** B864–B871
- [17] Khan S N and Eisenbach M 2016 *Physical Review B* **93** 024203
- [18] Kingma D P and Ba J L 2015 *Adam: a method for stochastic optimization*, (ICLR conference paper) arXiv:1412.6980
- [19] Kohn W and Sham L J 1965 *Physics Review* **140** A1133–A1138
- [20] McCulloch W and Pitts W 1943 *Bulletin of Mathematical Biophysics* **5** 115–133
- [21] Nightingale M P and Umrigar J C 1999 *Quantum Monte Carlo Methods in Physics and Chemistry* (Springer)
- [22] Rapaport D C 1996 D. C. RAPAPORT, *The Art of Molecular Dynamics Simulation*, (Cambridge University Press New York, NY, USA) ISBN:0521445612.
- [23] Rosenblatt F 1961 *Principles of Neurodynamics: Perceptrons and the Theory of Brain Mechanisms* (Spartan Books, Washington DC)
- [24] Rusu A A, Rabinowitz N C, Desjardins G, Soyer H, Kirkpatrick J, Kavukcuoglu K, Pascanu R and Hadsell R 2016 *Progressive neural networks*, arXiv:1606.04671v3
- [25] Ryczko K, Strubbe D and Tamblyn I 2019 *Phys. Rev. A* **100** 022512
- [26] Sholl D S and Steckel J A 2009 *Density functional theory: a practical introduction*, Chapter 1, (John Wiley and Sons, Inc. Publication) p. 12
- [27] Sinititskiy A V and Pande V S Deep Neural Network Computes Electron Densities and Energies of a Large Set of Organic Molecules Faster than Density Functional Theory (DFT), arXiv:1809.02723

- [28] Wang Y, Stocks G M, Shelton W A and Nicholson D M C 1995 *Physical Review Letters* **75** 2867–2870
- [29] Webb A M, Reynolds C, Iliescu D, Reeve H, Lujan M and Brown G 2019 Joint Training of Neural Network Ensembles, arXiv:1902.04422
- [30] <https://www.olcf.ornl.gov/for-users/system-user-guides/titan/>
- [31] Wang C, Tharval A and Kitchin J R 2018 *Molecular Simulations* **44** 623–630
- [32] Chen T and Guestrin C 2016 *The International Conference on Knowledge Discovery and Data Mining* DOI: <http://dx.doi.org/10.1145/2939672.2939785>.
- [33] *XGBoost Documentation* <https://xgboost.readthedocs.io/en/latest/>